



Age estimation of red snapper (*Lutjanus campechanus*) using FT-NIR spectroscopy: feasibility of application to production ageing for management

Michelle S. Passerotti ^{1*}, Thomas E. Helser², Irina M. Benson², Beverly K. Barnett³, Joseph C. Ballenger ⁴, Walter J. Bubley⁴, Marcel J. M. Reichert⁴, and Joseph M. Quattro⁵

¹Department of Biological Sciences, University of South Carolina, Columbia, SC 29208, USA

²Resource Ecology and Fisheries Management Division, Alaska Fisheries Science Center, National Marine Fisheries Service, NOAA, 7600 Sand Point Way NE, Seattle, WA 98115, USA

³Panama City Laboratory, Southeast Fisheries Science Center, National Marine Fisheries Service, 3500 Delwood Beach Road, Panama City, FL 32408, USA

⁴Marine Resources Research Institute, South Carolina Department of Natural Resources, Charleston, SC, USA

⁵School of the Earth, Ocean, and Environment, University of South Carolina, Columbia, SC 29208, USA

*Corresponding author: tel: +1 850 445 6636; e-mail: mpasserotti@gmail.com.

Passerotti, M. S., Helser, T. E., Benson, I. M., Barnett, B. K., Ballenger, J. C., Bubley, W. J., Reichert, M. J. M., and Quattro, J. M. Age estimation of red snapper (*Lutjanus campechanus*) using FT-NIR spectroscopy: feasibility of application to production ageing for management. – ICES Journal of Marine Science, doi:10.1093/icesjms/fsaa131.

Received 20 May 2020; revised 25 June 2020; accepted 1 July 2020.

Recent application of Fourier transform near infra-red spectroscopy (FT-NIRS) to predict age in fish otoliths has gained attention among fisheries managers as a potential alternative to costly production ageing of managed species. We assessed the age prediction capability of FT-NIRS scans in whole otoliths from red snapper, *Lutjanus campechanus*, collected from the US Gulf of Mexico and US Atlantic Ocean (South Atlantic). Otoliths were scanned with an FT-NIR spectrometer and resulting spectral signatures were regressed with traditionally estimated ages via partial least squares regression to produce calibration models, which were validated for predictive capability against test sets of otoliths. Calibration models successfully predicted age with R^2 ranging 0.94–0.95, mean squared error ≤ 1.8 years, and bias < 0.02 years. Percent agreement between FT-NIRS and traditional ages was lower than within-reader agreement for traditional estimates, but average percent error was similar and Kolmogorov–Smirnov tests were not significantly different ($p \geq 0.06$) between traditional and FT-NIRS predicted ages for optimal calibration models. Ages > 31 years were not well predicted, possibly due to light attenuation in the thickest otoliths. Our results suggest that FT-NIRS can improve efficiency in production ageing for fisheries management while maintaining data quality standards.

Keywords: age structure, light penetration, otolith chemistry, otolith thickness

Background

Age estimation of marine fishes for use in management is one of the costliest elements of the fisheries stock assessment process in terms of both money and time expenditures. In the United States, production ageing of hundreds of managed species is carried out

on a continuous basis by both federal and state agencies, often comprising numerous age readers and methodologies to compile estimates for hundreds of thousands of fish per year (Campana and Thorrold, 2001; Helser *et al.*, 2019a). Processing of ageing structures, usually otoliths, might entail embedding in resin, thin

sectioning, mounting sections on slides, and enumerations of growth bands by multiple readers to generate age estimates. The total time expenditure can average hours per specimen and be subject to reader bias on varying scales depending on the methodology, experience, and training of readers (Campana, 2001).

Fourier transform near infra-red spectroscopy (FT-NIRS) is a non-destructive light spectroscopy technique that has been used in agriculture and pharmaceuticals for several decades (Reich, 2005) and more recently has been applied to wildlife biology (Vance et al., 2016). FT-NIRS passes light from the near infra-red (NIR) region through a sample, and the interaction of this light with the sample over the length of the NIR spectrum forms a “spectral signature” of absorbance measurements at each wavelength (or wavenumber), which indicates the presence and quantity of organic chemical bonds contained within the sample, namely CH, –OH, –NH, and –SH (Murray and Williams, 1987; Williams, 2008). In biological applications, spectral signatures acquired from various species have been correlated with variables such as age in mosquitos (Mayagaya et al., 2009; Sikulu-Lord et al., 2016; Lambert et al., 2018), sex in frogs (Vance et al., 2014), and faecal content in mammals (Tolleson et al., 2005; Wiedower et al., 2012), enabling diagnostic tools for predicting these metrics based on spectral data alone.

Rapid age estimation in fish using FT-NIRS scans of whole ageing structures has the potential to revolutionize the way age estimates are produced for fisheries stock assessment (Wedding et al., 2014; Rigby et al., 2014, 2016; Robins et al., 2015; Helser et al., 2019a; Passerotti et al., 2020). Application of FT-NIRS technology to fish age estimation uses a calibration set of otoliths with associated traditionally estimated ages to “train” a predictive model using NIR spectral data as a response. The set of spectral data is then evaluated using multivariate partial least squares (PLS) regression to correlate spectral signatures with age. This process produces a linear correlation model to predict the age of a fish based on a rapid scan (usually ≤ 60 s) of a whole otolith. Ideally, the calibration model should incorporate as much age-related spectral variation as possible, so that its subsequent prediction ability is robust. To evaluate the predictive capability of the calibration model, both an internal cross-validation and an external validation using a separate test set of otoliths are ideal (Williams, 2008). The potential impact of this technology on the production ageing process for fisheries stock assessment, both in turnaround time and cost, is significant (Robins et al., 2015; Helser et al., 2019a). To this end, US federal management entities are actively vetting the incorporation of FT-NIRS into current stock assessment processes (Helser et al., 2019b) and recommendations have been made to pursue the use of FT-NIRS for improving the scope and timing of production ageing for managed species (SEDAR, 2020).

While published FT-NIRS age estimates suggest prediction error rates similar to traditional age estimation, further comparison of FT-NIRS predicted ages to traditional ages in the context of age data products used in fisheries stock assessment models has not been published. Comparisons of percent agreement (PA) and bias from FT-NIRS-acquired data and traditional age readers are similar in scale and have been reported by Helser et al. (2019a) and Rigby et al. (2014, 2016). Similarly, Rigby et al. (2016) and Passerotti et al. (2020) used FT-NIRS predicted ages to create growth models for comparison to traditional age-length data. Further translation of FT-NIRS ages, for example to age composition for use in catch-at age models, has not been published. In

addition, basic information as it relates to the physical properties of ageing structures interrogated by the approach (for instance, depth of NIR light penetration) is lacking.

Red snapper *Lutjanus campechanus* are a long-lived (50+ years) sub-tropical reef fish species found in the western Atlantic Ocean and throughout the Gulf of Mexico (GOM) (Manooch and Potts, 1997; Nelson and Manooch, 1982) for which ageing methods have been validated with the bomb radiocarbon $\Delta^{14}\text{C}$ chronometer (Baker and Wilson, 2001; Barnett et al., 2018; Andrews et al., 2019). In the southeastern United States, it is one of the most commercially and recreationally important marine finfish species, accounting annually for over \$20 million in commercial landings and nearly \$50 million in economic impacts from the recreational fishery, mostly in the US GOM [NMFS (National Marine Fisheries Service), 2018]. This species is federally managed as two separate stocks, the US GOM and southern US Atlantic Ocean [South Atlantic (SA)], with the GOM stock further subdivided into eastern and western subunits with a line of demarcation at the Mississippi River (Figure 1, modified from SEDAR, 2008). The regulatory history of red snapper has been complex, contentious, and costly (Cowan, 2011), requiring a large investment of effort and time to collect and process increasing numbers of biological samples to be used as assessment model inputs. In the most recent GOM red snapper stock assessment (SEDAR 52; SEDAR, 2018), nearly 50 000 new age estimates were produced over 4 years from fish collected from the US GOM region alone (Lombardi, 2017) at an enormous cost in terms of time and money. Though fewer red snapper are collected in the Atlantic region [NMFS (National Marine Fisheries Service), 2018; SEDAR, 2017], over 10 000 SA ages have been produced in the last 5 years (M. Reichert, pers. comm.).

Given the high costs of producing age estimates on the scale and timeline needed for the management of red snapper, and the potential of FT-NIRS to generate ages for use in management, we evaluated the capability of FT-NIRS to predict age from whole otoliths of red snapper in the context of production ageing across regional stocks. Furthermore, we report novel experimental results evaluating the depth of NIR light penetration in otoliths of varying size and age, which has not been previously documented but represents a necessary step forward to determining the physical focus (or foci) of the NIRS/age correlation.

Methods

Sample selection

Sagittal otolith samples used in this study were compiled from archival fishery-independent collections of red snapper collected from the US GOM and southeastern US Atlantic Ocean (SA). GOM samples were collected for the NOAA Southeast Fisheries Science Center, Panama City Laboratory, and herein are further subdivided into eastern GOM (EGOM) and western GOM (WGOM) sample sets according to catch location and geographic designations for subunits of the GOM stock as defined by federal stock assessments (SEDAR, 2008; Figure 1). SA samples were collected by the South Carolina Department of Natural Resources (SCDNR), Marine Resources Research Institute, as part of the Southeast Reef Fish Survey and Marine Resources Monitoring Assessment and Prediction sampling programmes. Generally, fishery-independent sources collect both right and left sagittal otoliths; left otoliths are typically sectioned for ageing, leaving the right otolith available for FT-NIRS. For this study, otoliths were

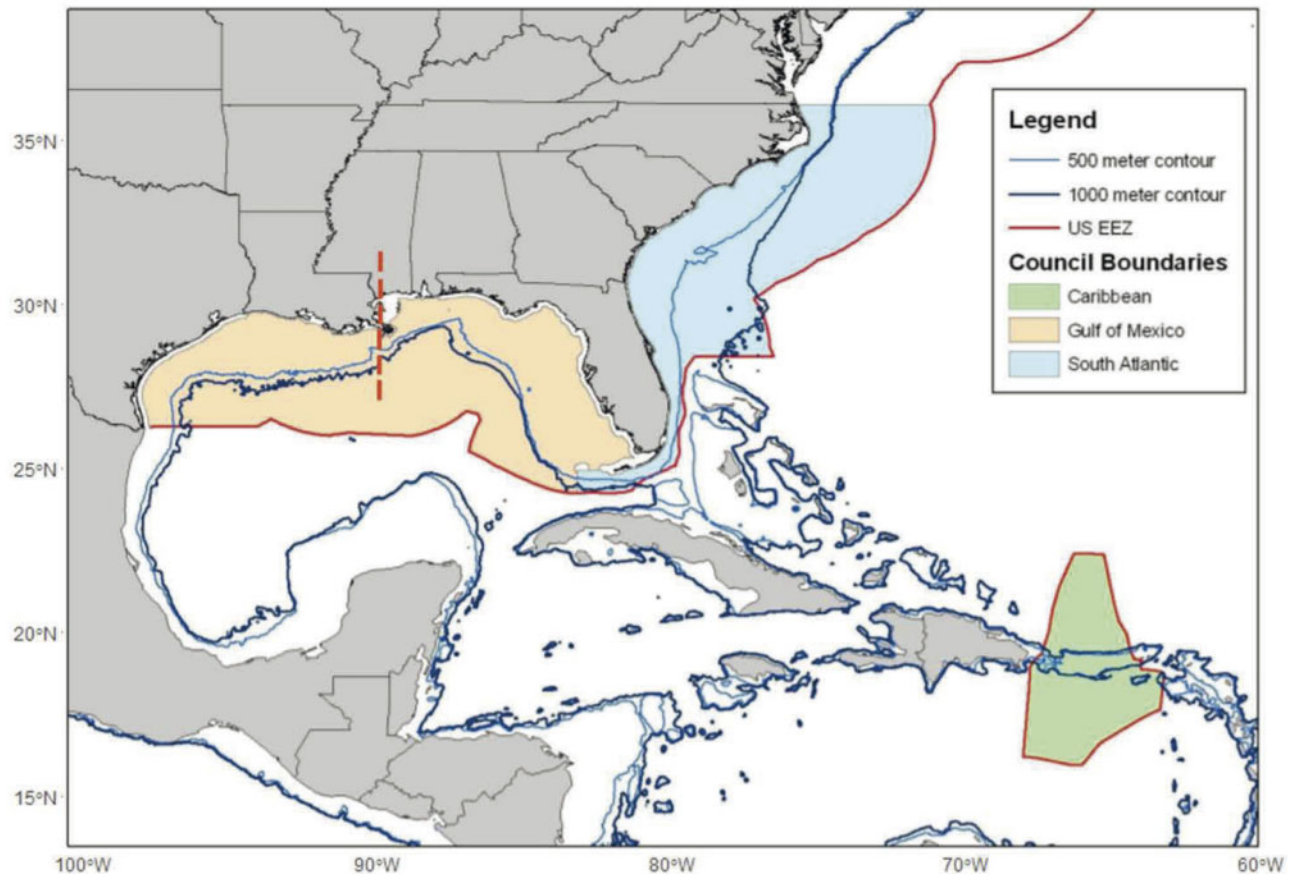


Figure 1. US federal management regions for red snapper, adapted from SEDAR (2008). The GOM is divided into eastern (EGOM) and western (WGOM) subunits roughly along the Mississippi River boundary as indicated by the orange dashed line. Samples for this study were grouped into three regions for testing: EGOM, WGOM, and South Atlantic.

selected to equalize sample sizes across regions while maintaining a similar range of collection years (GOM: 2011–2016, SA: 2011–2017). A notable exception was the inclusion of the two oldest otoliths aged 35 and 38 years, both from the SA. These otoliths were collected in 1997, but because otoliths of advanced age (generally 30+) were not available within the constrained collection years, we included them for the evaluation of FT-NIRS age prediction for long-lived individuals.

We selected separate calibration and test sets of otoliths from each geographic region for comparison: EGOM, WGOM, and SA. Calibration sets were selected to approximate a uniform distribution within regions, with relatively even numbers of samples ($n \sim 10$ per age class) across all available age classes, where possible. Test sets of otoliths for each region were chosen at random from the same sampling years to mirror a typical age structure for each population (Figure 2). Otoliths were stored dry in coin envelopes after collection and were wiped clean with ethanol and air dried for at least 48 hr prior to FT-NIR data acquisition.

Traditional age estimation

For each otolith used in the FT-NIRS analysis, a traditional calendar age estimate, or reference value, was available from the paired otolith and was generated using methods as outlined in SEDAR (2015) for GOM otoliths and in Wyanski *et al.* (2015) for SA otoliths. All otoliths were independently aged by at least two age

readers. Only those ages obtaining consensus were included in this analysis. For GOM age estimates, three independent age readings were available for each otolith and only estimates where at least two of three counts agreed were used. For SA age estimates, two age readers performed independent counts, and for those that did not initially agree, consensus was subsequently obtained or else the sample was excluded from the analysis. Because red snapper are protracted spawners, calculation of calendar age requires information on increment count (i.e. number of annuli), month of capture, edge type, and month of increment formation using the conditional formula (Potts, 2009; Allman *et al.*, 2012):

$$\text{Calendar age} = \begin{cases} \text{increment \#} & \text{month} \geq \text{July} \\ \text{increment \#} & \text{month} < \text{July and narrow translucent edge} \\ \text{increment \#} + 1 & \text{month} < \text{July and wide translucent edge.} \end{cases}$$

Spectral data collection

Spectral data were collected with a Bruker Matrix I FT-NIR spectrometer (Bruker Scientific, Billerica, MA, USA). Whole otoliths were positioned convex-side down in the middle of the sample

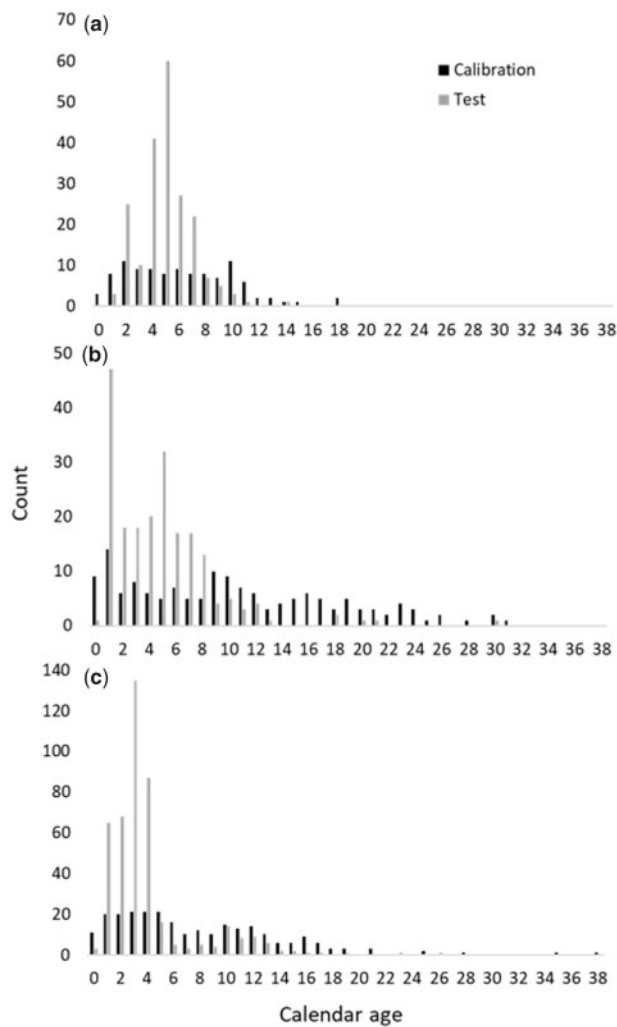


Figure 2. Red snapper sample age distributions for calibration and test sets for the (a) EGOM, (b) WGOM, and (c) SA.

window with the rostral axis positioned horizontally relative to the sample window (see [Robins et al., 2015](#), for detailed description and pictures of scanning setup). A gold-coated transreflectance cap was placed over the top of the otolith to reduce stray light entering the detector. A total of 64 spectral scans were acquired for each otolith at a frequency of 16 cm^{-1} along the entire NIR spectrum ($3600\text{--}12\,000\text{ cm}^{-1}$), and scans were averaged to produce a single representative spectrogram for each sample. Each spectrogram took approximately 30 s to produce. Principle components analysis (PCA) was used for data visualization and outlier detection within the PLS regression process. Spectral data analysis was conducted using the OPUS software suite (version 7.8; Bruker Scientific, Billerica, MA, USA).

Data preprocessing and model selection

For each calibration model, multivariate spectral data were fitted to traditionally estimated otolith ages using PLS regression ([Chen and Wang, 2001](#)). Models were evaluated for age prediction capability using a “leave one out” method of cross-validation, whereby calibration models were produced with one or more samples left out and those samples subsequently tested against the model for

goodness of fit. This was repeated, in turn, with each sample tested against its calibration model until all samples had been cross-validated and goodness of fit was judged based on the R^2 (coefficient of determination), root mean square error of cross-validation (RMSECV), and residual prediction deviation (RPD) values. RPD values of 3 or higher are generally accepted as “good” from a chemometrics standpoint ([Williams, 2008](#)). Wavenumber selection and data preprocessing treatments were compared to determine treatments and wavenumber ranges that minimized the RMSECV of predicted ages, resulting in an optimized model capable of generating FT-NIRS-predicted ages from spectral data alone. Loadings plots were evaluated and noisy regions of the spectrum were excluded to yield optimized wavenumber selection. In addition to standalone regional calibration models (EGOM, WGOM, SA), we tested combined GOM (WGOM and EGOM) and All Regions Combined (WGOM, EGOM, and SA combined) calibrations. Once final calibration models were chosen for each region, calendar ages for test sets of otoliths were predicted by each calibration model, in turn, and model fits compared to determine the optimal prediction model for each test set. We also calculated % root mean square error (% RMSE) = $(\text{RMSE}/\text{maximum age} \times 100)$ to evaluate standardized model error in the context of the maximum age included in the model ([Couture et al., 2016](#); [Passerotti et al., 2020](#)).

Samples in the oldest age classes were underrepresented as our pooled samples contained only two samples beyond 31 years. In forming calibration models, including these rare, older otoliths in the SA and All Regions Combined models caused differences in both model performance and in the preprocessing required to yield optimum age prediction. This could be due to one or more factors: the different collection year for older otoliths, some physical or chemical difference in the otolith-NIR light interaction for these samples or simply reduced model performance due to the inconsistency of sample distribution. As such, we compared optimized calibration models that either included (“SA Complete” and “All Regions Complete”) or did not include (“SA Truncated” and “All Regions Truncated”) the oldest two samples to assess how their inclusion affected the subsequent models’ predictive capability. For all models except the two “Complete” models, spectral data were preprocessed by mean-centring followed by transformation using the Savitsky–Golay first derivative with 17 smoothing points (polynomial order = 2), which corrects for baseline shifts due to light scatter from differences in particle size and perhaps other physical differences among samples. “Complete” models, those including the two oldest fish, were optimized using only wavelength selection with no further preprocessing, as this data treatment yielded better model results than any preprocessing regime in which spectral data were transformed.

Bias estimates

Relative bias was compared between FT-NIRS predicted ages and traditional age estimates (FT-NIRS bias), as well as between individual reader ages comprising the traditional age estimates (reader bias). FT-NIRS ages predicted from calibration models are produced as continuous numbers rather than integer ages; hence, comparison of calendar age estimates between methods required rounding raw FT-NIRS ages to the nearest integer. Relative bias (B) was calculated for FT-NIRS ages as $B^{\text{FT-NIRS}} = \text{Age}^{\text{FT-NIRS}} - \text{Age}^{\text{Traditional}}$ and for traditional ages as $B^{\text{Trad}} =$

$\text{Age}^{\text{Reader1}} - \text{Age}^{\text{Reader2}}$ (Helser *et al.*, 2019a). PA and average percent error (APE; Beamish and Fournier, 1981) were calculated for both types of ages for comparison using the FSA package in R (Ogle *et al.*, 2018). To further evaluate the capability of FT-NIRS to generate age compositions similar to those used to inform management, we tested for differences ($\alpha = 0.05$) in test-set sample age distributions derived from FT-NIRS predicted- and traditional-age data using a two-sided Kolmogorov–Smirnov (K–S) test on ages output for each test/calibration set combination.

Light penetration

Given the differences in model performance and preprocessing requirements for the oldest samples, and the constraint given sample availability that we could not experimentally change collection year or sample distribution to test for their effects on model performance, we chose to evaluate whether NIR light penetration is attenuated in older, thicker otoliths, which could lead to age underestimation and differences in preprocessing requirements for best predicting age in these otoliths. We selected a subset of 58 otoliths from the SA ranging 1–38 years in age, measured thickness of the otoliths through the core region using callipers, and tested for a distinct chemical signature (polystyrene) on the distal concave surface of the whole otolith as detected by NIR light penetration through the otolith core. Otoliths were positioned on the sample window as previously described and a 5-mm diameter polystyrene disc was placed on top of the otolith, directly over the core area. Polystyrene was chosen because it provides a distinct FT-NIR signature detectable even in the presence of otolith signatures. Otoliths were scanned as described earlier and spectra were evaluated for differences in signatures with and without polystyrene. Spectra were transformed using a Savitsky–Golay first derivative with 17 smoothing points (polynomial order = 2), and wavelength range was reduced to select the regions where the polystyrene spectral signature was most easily differentiated from that of otoliths based on their respective individual signatures. PCA was used to discriminate the presence or absence of a polystyrene signature. Analyses were carried out using the Conformity package within OPUS (version 7.8) and The Unscrambler 10.2 (Camo Analytics).

Results

A total of 1357 otoliths were included in FT-NIR age prediction analyses across all regions (WGOM: $n = 354$, EGOM: $n = 311$, SA: $n = 692$). PCA of preprocessed spectral data for all otoliths showed no discernible separation due to region (Figure 3a). The first two principle components (PCs) explained 98% of the spectral variation among otoliths; in contrast, the first two PCs explained only 84% of the spectral variation among age groups (Figure 3b). Most FT-NIRS age calibration models required 6–8 PCs (model rank) to maximize predictive power (Table 1), suggesting that spectral differences explaining <2% of the overall variance played a substantial role in successful age prediction.

All calibration models performed well, predicting traditional calendar age with $R^2 = 0.94$ – 0.95 , RMSECV ≤ 1.8 years, bias < 0.02 , and RPD > 4 (Table 1 and Figure 4). Although some differences in prediction capability were apparent among regional calibrations, the All Regions Combined models generally performed at or above the level of the regional models and predicted age to within about 1.5 years with minimal bias and favorable RPD scores. In addition, % RMSE for the All Regions Combined

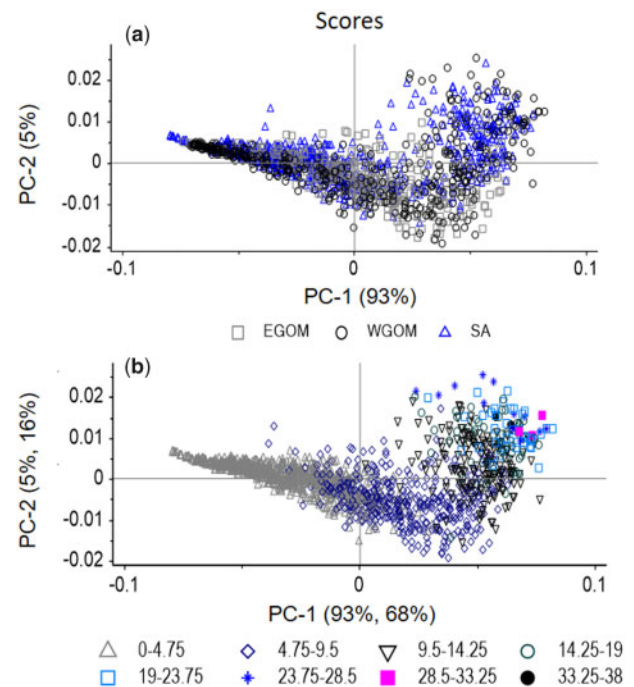


Figure 3. PCA of first-derivative transformed spectral data for all red snapper otoliths coded by (a) region and (b) age group. Additional scores for PCs in 3B correspond to the first two factors of a combined region age prediction model explaining 68 and 16% of variation in predicted calendar ages.

Complete model was lower than nearly all other calibrations, owing to the larger age range included in the Complete models. Informative spectra did exhibit some variation between the two regions but overall were similar to each other in range (Figure 5).

The lack of regional spectral differentiation and the equivalence of calibration models are compelling; hence, for clarity and brevity, we will discuss test-set results for all regions combined as predicted by the All Regions Combined calibration models only, although full results from pairwise validation of regional test-set/calibration model combinations are provided in Supplementary Table S1 for reference. Combined test-set ages were predicted well by both All Regions Combined models, with $R^2 = 0.92$ and root mean square error of prediction (RMSEP) ~ 1.00 , meaning that at least 67% of ages were predicted to within a year or less relative to traditional age (Table 2 and Figure 6). Of the two models, the All Regions Truncated calibration optimized all parameters for combined test-set ages.

Bias between FT-NIRS and traditional ages was similar overall for all test sets (Table 2 and Supplementary Table S1); therefore, only results for the All Regions Truncated model are plotted. Mean FT-NIR bias \pm SD by age class overlapped reader bias across most ages (Figure 7). FT-NIRS bias increased at older ages over that of traditional age estimates, but otherwise mean bias was equivalent between ageing methods. Overall, PA was lower for FT-NIRS ages relative to between-reader agreement for traditional ages (Figure 8), with FT-NIRS PA ± 1 year = 87.1% and traditional between-reader PA ± 1 year = 93.4%. Between-reader APE varied by region (GOM = 4.71%, SA = 9.70%, Combined = 6.97%) and was lower than FT-NIRS-generated values (Table 2 and Supplementary Table S1). Age distribution of FT-NIRS ages

Table 1. Calibration model results for red snapper FT-NIRS age prediction, by region.

Calibration model (calendar age)	<i>n</i>	Maximum age	Rank	<i>R</i> ²	RMSECV	% RMSE	Bias	RPD	Slope	Offset
WGOM	150	31	6	0.94	1.84	5.94	−0.002	4.16	0.95	0.56
EGOM	105	18	4	0.95	0.85	4.72	0.009	4.67	0.95	0.31
GOM Combined	255	31	6	0.94	1.6	5.16	0.000	4.14	0.94	0.50
SA Truncated	253	28	8	0.94	1.35	4.82	0.019	4.12	0.95	0.38
SA Complete*	255	38	8	0.94	1.52	4.00	0.011	4.02	0.94	0.49
All Regions Combined Truncated	508	31	8	0.94	1.54	4.97	−0.004	4.02	0.94	0.49
All Regions Combined Complete*	510	38	9	0.94	1.58	4.16	0.001	4.06	0.94	0.51

The “Complete” models for SA and All Regions Combined (indicated by *) are those including the two oldest fish in the study aged 35 and 38 years, while “truncated” models exclude these samples.

did not differ significantly from that of traditional ages for validations where RMSEP was minimized and PA maximized (Table 2, Supplementary Table S1, and Figure 9). For nearly all test sets, this corresponded to validation with the All Regions Truncated calibration model. Combined test-set ages predicted with the All Regions Complete calibration were significantly different than traditional estimates ($p = 0.004$).

Light penetration

Ages up to 38 years were cross-validated in the SA Complete and All Regions Combined Complete calibration models, comprising the oldest otoliths assessed for FT-NIR age estimation to date, and the lowest % RMSE for annually aged otolith calibrations published to date (Table 1 and Figure 4e and g; Passerotti et al., 2020). Optimization of Complete age prediction models was achieved using raw spectral data, that is spectral data that had undergone no data transformations or smoothing algorithms (pre-processing). Conversely, all other models presented were optimized using mean-centring and first derivative Savitsky–Golay transformations. Preprocessed Complete calibration models were characterized by higher offset (SA: 0.70, All Regions: 0.59), lower slope (SA: 0.90, All Regions: 0.93), reduced RMSECV (SA: 1.68, All Regions: 1.67), and greater bias at age classes ≥ 28 years (i.e. mean bias \pm SD: SA preprocessed = 7.1 ± 3.6 years, SA no preprocessing = 4.3 ± 3.1 years) relative to the un-preprocessed models ultimately used for cross-validation (Table 1). Despite excellent predictive ability based on PLS regression model metrics, ages of the oldest two otoliths (35 and 38 years old) were under-predicted in both Complete calibration models, in the SA Complete by 7.9 and 4.5 years and All Regions Complete by 6.6 and 3.3 years, respectively. Given that these un-preprocessed models used physical differences in light scatter to improve predictive capability, light penetration may have played a role in FT-NIR age prediction of the 35—and 38—year-old otoliths.

Otolith thickness ranged from 2.1 to 5.9 mm and increased with age (Figure 10). Raw spectra for otoliths both with and without the polystyrene disc, as well as the raw spectrum for polystyrene, are plotted in Figure 11a. The polystyrene spectrum has a unique and characteristic peak at 5950 cm^{-1} , which is easily discernable relative to the typical otolith spectrum in both position and magnitude. Generally, otolith spectra increase in magnitude with increasing fish age (although not absolutely), and the polystyrene signal at 5950 cm^{-1} became attenuated as the magnitude

of raw spectra increased. Preprocessing improved spectral differentiation between treatments (Figure 11b), and a PCA of preprocessed spectra by treatment is presented in Figure 12. Differentiation is apparent between disc and no-disc spectra, except for SA239, the 38-year-old fish with the thickest otolith, for which the “disc” spectrum overlaps the “no-disc” grouping as segregated along PC 1. While there was some separation of SA239 disc vs. SA239 no-disc scores, the fact that the SA239 disc spectrum could not be distinguished from other no-disc scores suggests the polystyrene signal is not detectable; hence, NIR light penetration is likely attenuated in this otolith.

Discussion

These results provide a baseline of understanding for the application of FT-NIRS to otolith age prediction across multiple stocks of red snapper and make a compelling case for the feasibility of incorporating FT-NIRS estimated ages into fish stock assessments for management. Calibration models predicted ages that were highly correlated to and within a year or less for the majority of test-set samples relative to traditionally estimated ages in fish ranging 0–31 years, lending further credibility to the use of FT-NIRS for ageing based on the example of shorter-lived pollock in Helser et al. (2019a). When translated into error terms more typically associated with age estimation error in fisheries, absolute PA for red snapper FT-NIRS predicted ages ranged 43–53%, with PA within ± 1 year of 87–89% and APE values $\leq 10\%$ relative to traditional ages. While PA was lower than most published between-reader values (i.e., Baker and Wilson, 2001; Wilson and Nieland, 2001; White and Palmer, 2004), PA ± 1 -year herein approached the $\sim 90\% \pm 1$ -year agreement reported for sub-sampled production ages in the GOM (Allman et al., 2002). APE values were typical relative to between-reader error in production ageing. In many cases for typical production ageing in the GOM, only one age estimate might be generated for an otolith due to time constraints. As such, the only measure of error for a given set of production ages might be those derived from counts of reference collections shared between ageing facilities. In the most recent assessment (SEDAR 52; SEDAR, 2018), a GOM reference collection was reported to have within-laboratory APEs ranging 1–7% for ageing facilities across the region (Lombardi, 2017) and APEs ranging 2.5–11.6% were reported in other calibration studies of the region (Allman et al., 2002, 2005). A similar reference collection of Atlantic red snapper otoliths aged across three production ageing laboratories produced an APE of $\sim 11\%$

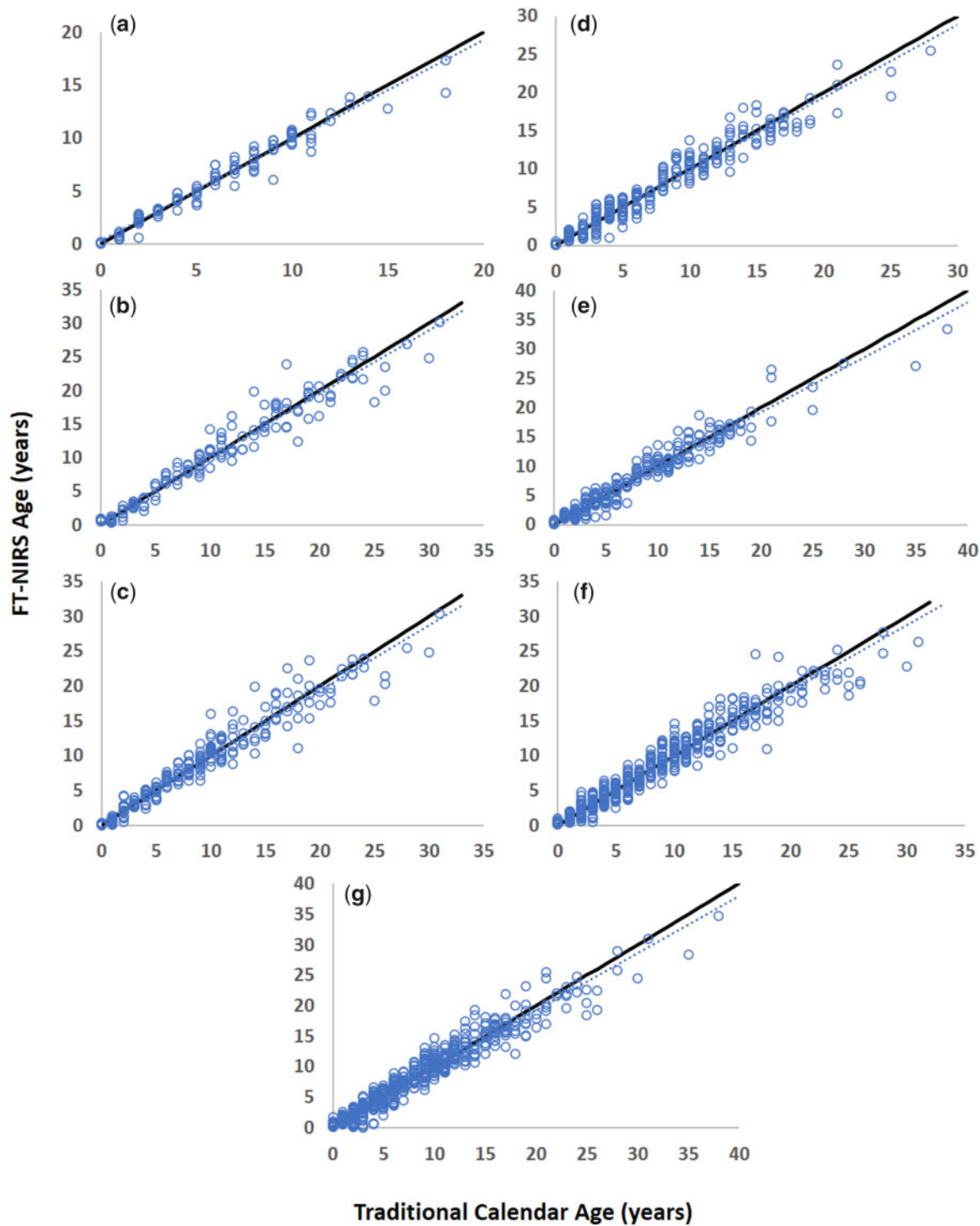


Figure 4. Plots of red snapper FT-NIRS age calibration model results for the (a) EGOM, (b) WGOM, (c) GOM combined, (d) SA Truncated, (e) SA Complete, (f) All Regions Combined Truncated, and (g) All Regions Combined Complete calibrations. Dashed line is the linear regression, and solid line represents a 1:1 regression line.

[SFB NMFS (Sustainable Fisheries Branch—National Marine Fisheries Service), 2015]. Because we only used otoliths with available consensus ages for this study, bias estimates for traditional ages herein are likely underestimated relative to ages typically supplied for management. Furthermore, age class distribution was not significantly different for FT-NIRS ages

relative to traditional estimates, which solidifies the potential use of FT-NIRS ages to generate stock assessment information such as mortality estimates. In all, FT-NIRS shows overt promise to improve efficiency in production ageing for fisheries management by greatly reducing time and effort while maintaining data quality standards.

Improvements in efficiency for FT-NIRS age estimation over traditional methods are substantial, particularly because as long as otoliths are clean and dried to ambient conditions, little preparation is required to collect spectral data (Robins *et al.*, 2015). In contrast, traditional age estimation protocols for red snapper require thin sectioning, mounting, and polishing of sections before band enumeration can be performed (VanderKooy, 2009). Realistically, a few hundred otoliths can be processed and aged in a typical work week using traditional methods. With FT-NIRS, each scan takes ~ 30 s using the spectrometer and settings in the current study. Depending on the set-up of the scanning system, manipulating samples on and off the spectrometer can add about 1 additional minute. Under optimized efficiency, spectral data collection for the 1357 otoliths analysed in this study could be accomplished in 34 hr. Some spectrometers have sample wheels that can be automated to rotate a series of samples over the sample window, which might further improve the efficiency of scanning. [Robins *et al.* (2015) provide more details regarding spectrometer cost and set-up options.] Model building and selection of optimum calibration models based on reference collections add additional time considerations to implementation of the FT-NIRS method. Because outcomes benefit from having calibration models encompassing the full range of spectral variability possible, one potential scenario for operationalizing FT-NIRS might be to scan all archival specimens to develop initial optimized calibrations on a species/region/temporal case-by-case basis and then re-evaluate models on a rolling basis as new years of otolith collections are added. Estimating ages traditionally for a subset of

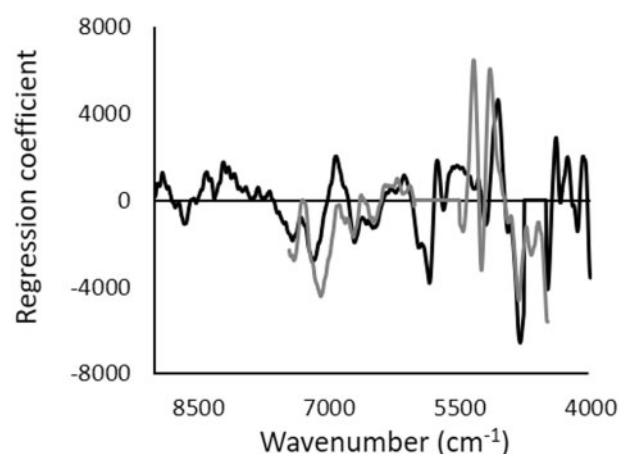


Figure 5. Loadings plot of regression coefficients for the GOM Combined (grey) and SA Truncated (black) age calibration models for red snapper.

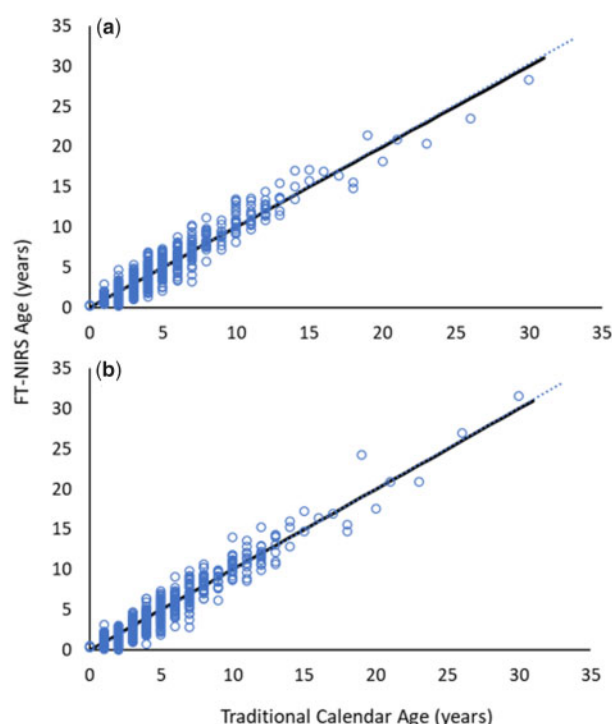


Figure 6. Plot of red snapper FT-NIRS test-set results for the (a) all regions (All Regions Truncated) and (b) all regions (All Regions Complete) validations. Dashed line is the linear regression, and solid line represents a 1:1 regression line.

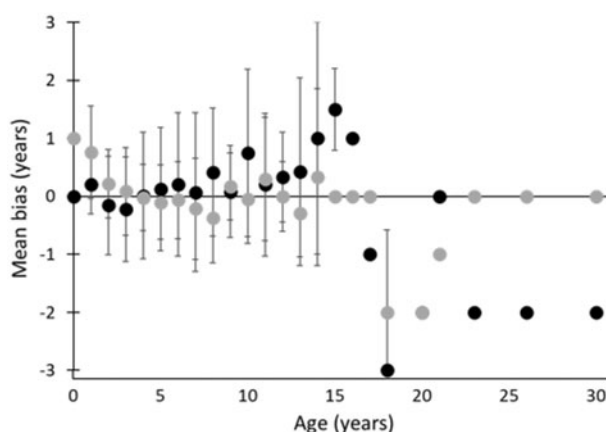


Figure 7. Mean bias \pm SD for red snapper FT-NIRS (black circles) and traditional (grey circles) ages by age class for all test sets combined, as predicted by the All Regions Combined Truncated calibration model.

Table 2. Validation results for the age prediction of regional test sets of red snapper otoliths relative to the corresponding calibration model used to test (in parentheses).

Test set (calibration tested against)	<i>n</i>	Maximum age	<i>R</i> ²	RMSEP	% RMSE	Bias	RPD	Slope	Offset	PA	APE	K-S <i>D</i>	<i>p</i>
All Regions Combined (All Regions Truncated)	847	30	0.92	0.99	3.30	-0.04	3.32	1.01	-0.01	45.8	10.4	0.07	0.056
All Regions Combined (All Regions Complete)	847	30	0.92	1.02	3.40	0.16	3.29	1.01	0.22	44.2	11.3	0.09	0.004

PA, APE, and results of two-sided K-S tests (*D* statistic and *p*-value) are also given for each test-set/calibration model combination.

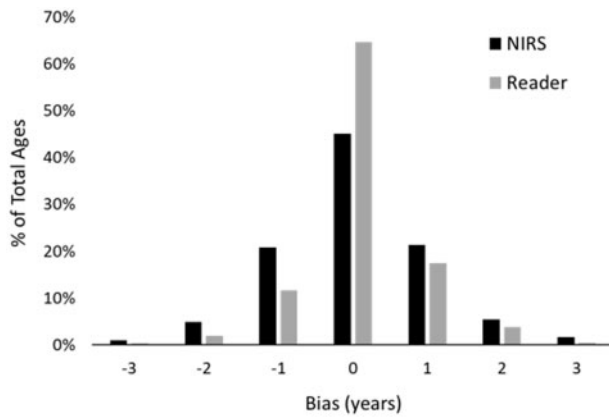


Figure 8. Frequency of relative bias (B) by method for all red snapper ages across all test sets combined as predicted by the All Regions Truncated calibration model. Raw FT-NIRS ages were rounded to the nearest integer before bias calculation to facilitate comparison with traditional ages.

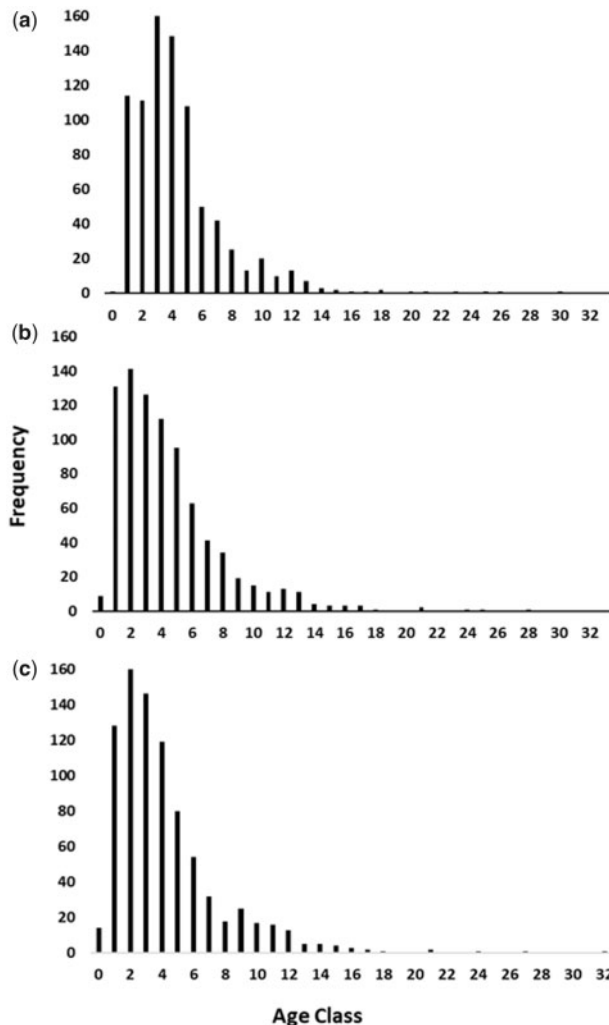


Figure 9. Age distributions for all red snapper test-set samples using (a) traditional ages and FT-NIRS predicted ages output by the (b) All Regions Combined Truncated and (c) All Regions Combined Complete calibration models.

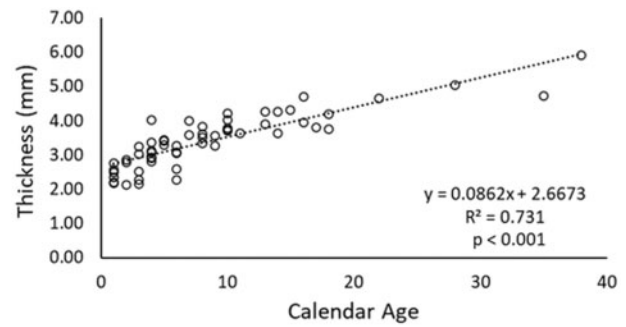


Figure 10. Otolith thickness (mm) at age (years) for 58 red snapper otoliths assessed for NIR light penetration.

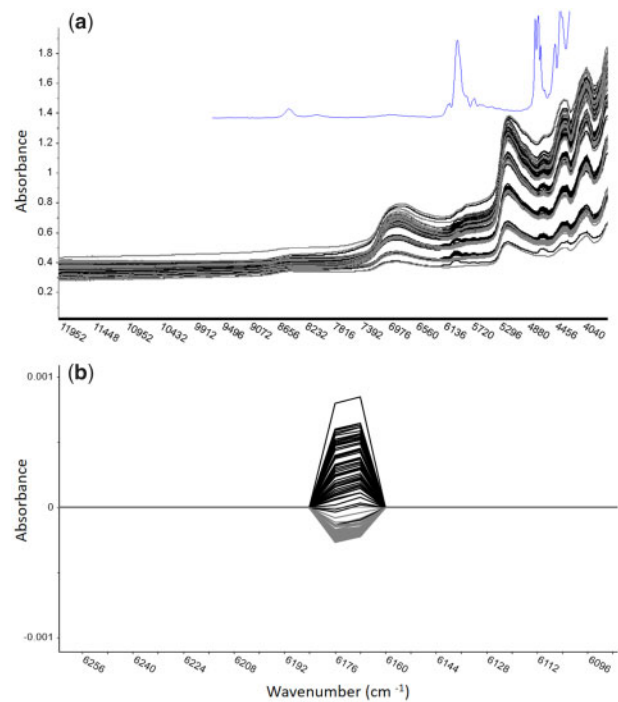


Figure 11. Raw (a) and first-derivative transformed (b) spectra of red snapper otoliths scanned for light penetration trial with no disc (grey) and polystyrene disc (black). The raw spectrum for polystyrene is overlaid in blue in (a). Differentiation was judged based on wavenumber range 6280–6080.

collections each year would provide calibration data for model comparisons and create a checkpoint for quality control.

Current understanding of the underlying drivers of FT-NIRS age prediction is lacking, but it has been suggested that age-related changes to the otolith protein or organic matrix are a likely mechanism (Helser *et al.*, 2019a). Red snapper age prediction models generally relied on spectral regions between 7600 and 4100 cm^{-1} , a reduced region relative to the entire spectrum interrogated (12 000–4000 cm^{-1}), with some model-specific variation in the importance of different signals occurring throughout that range. These reduced regions roughly correspond to various –CH, –OH, and –NH bonds and are similar to important age-predictive regions from other otolith age prediction models (Wedding *et al.*, 2014; Robins *et al.*, 2015; Helser *et al.*, 2019a).

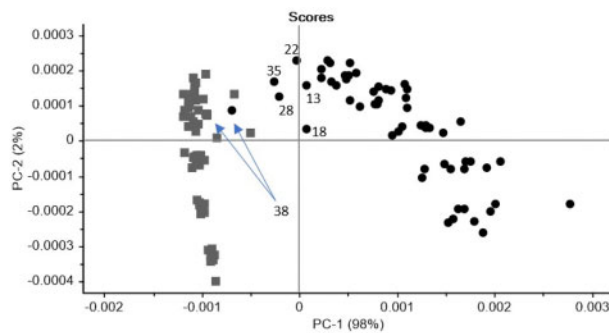


Figure 12. PCA of red snapper otolith light penetration spectra with no disc (grey squares) and polystyrene disc (black circles). Selected proximal “disc” samples are labelled with age to show spatial trends.

including juvenile red snapper (Passerotti *et al.*, 2020). Ostensibly, otoliths record variability in both environment and fish physiology, and chemical changes might be associated with the crystal lattice, deposition of the organic layer, or both, depending on the molecule (i.e. Campana, 1999; Izzo *et al.*, 2016; Thomas *et al.*, 2017; Thomas and Swearer, 2019). The assumption that FT-NIRS detects all chemical changes and that the changes are definable with age requires further confirmation. Environment and physiology can interact with otolith morphometrics to create spatial heterogeneity in otolith chemistry within individual structures (Sturrock *et al.*, 2015; Limburg and Elfman, 2017; Vasconcelos-Filho *et al.*, 2019), which could also play a role in age-related patterns in FT-NIRS signatures. Further work is needed to define age-related physicochemical patterns in otoliths as related to changes in the FT-NIRS signature.

Region did not explain most of the variation in otolith spectral signatures based on PCA, although age prediction model outcomes did vary by region. Hence, the regional differences in calibration model performance likely stem from an interaction of regional differences in sample size and ageing precision for traditional reference ages, and temporal variation included in the growth history of otoliths. Environmental variability between regions could also play a role in regional model performance, despite best efforts to minimize this by constraining of sampling years. The SA sample sets included an additional year of collections (2017) as well as the two oldest otoliths collected in 1997, which might have added variability not accounted for by the GOM samples. Preliminary analysis of GOM red snapper showed that RMSEP was lower in a single year (2012) calibration than for multiple years combined (Barnett *et al.*, 2019), although this is based on a small sample size. For some test-set validations herein, age prediction improved when spatial variability and sample size of the calibration model increased (Supplementary Table S1) and the All Regions Truncated model optimized RMSEP and PA in most test sets. All other published studies have found similar evidence. Helser *et al.* (2019a) found similar results in walleye pollock *Gadus chalcogrammus*, where some annual and regional variation in spectral data was evident, but combined year models performed best when considering test-set results across all groupings. Wedding *et al.* (2014) and Robins *et al.* (2015) also found seasonal and geographic differences in spectral signatures and resulting age calibration models for coastal snapper and barramundi species and again found it preferable to combine

calibrations to accommodate variation for optimizing prediction capability. Studies of red snapper otolith chemistry have found regional differences in stable isotope and trace element profiles within the GOM (Patterson *et al.*, 2008; Nowling *et al.*, 2011; Sluis *et al.*, 2012, 2015; Zapp Sluis *et al.*, 2013) and the Atlantic (Barnett *et al.*, 2016), but no comparative studies between the GOM and Atlantic exist. Further chemical profiles of otoliths from both regions are lacking. In addition, while trace elements can be bound to organic matrix in otoliths (Izzo *et al.*, 2016; Thomas *et al.*, 2017; Thomas and Swearer, 2019), it is not clear whether FT-NIRS can detect trace elements in otoliths, although the lack of regional spectral variation suggests that they are not detectable at a diagnostic level in whole otoliths.

In addition to spatial and temporal variation among spectra, the age structure of sample sets varied across regions despite efforts to standardize that of calibration sets. Constraining the collection years included in calibration models might control for some temporal variation in water quality and other environmental variables; however, the age composition of sample sets will inherently affect the temporal variability included in the model since otoliths from older fish include more years of environmental variation than do those from younger fish. For populations with mostly young fish, e.g. EGOM, modelled variation might differ significantly from populations with older fish sampled in the same years and in the absence of regional variability. This idea has potential ramifications for ages estimated from single-gear surveys, where gear biases in catch-at-size by age might affect age distributions and thus any resulting FT-NIRS calibration models. Future effort should include the collection of FT-NIRS data for all archived otoliths to further explore dynamics in spectral variation across time and regions, as well as the effects of age distribution on model performance.

Model performance in terms of PA, APE, and age composition presented herein relative to the PLS regression metrics typically reported in FT-NIRS feasibility studies demonstrates that additional considerations are necessary to select optimal calibration models for otolith age data. Despite satisfactory model performance for nearly all models presented here based on R^2 , RMSEP, and RPD values as defined in previous FT-NIRS age prediction studies (Wedding *et al.*, 2014; Rigby *et al.*, 2014, 2016; Robins *et al.*, 2015; Helser *et al.*, 2019a; Passerotti *et al.*, 2020), the resulting translation to integer ages for management use did not always yield optimal PA and APE values (Supplementary Table S1), which are typically used to judge quality of age estimates in fisheries research. Differences among prediction performance metrics might stem from the rounding convention used to transform the decimal ages output from FT-NIRS prediction models to integers for use as calendar ages. We compared several rounding methods and found none worked better than conventional rounding; however, further investigation into best practices might very well lead to improvements in this area. There might also be some “regression effect” or “regression towards the mean” occurring differentially among calibration/test-set pairings, whereby the mean age of the calibration model, and thus the age for which model prediction error is least, differs from that of the test set, thereby increasing prediction error disproportionately in age classes as they progress sequentially further from the calibration model mean (Williams, 2013). Regional differences in otolith chemistry aside, this regression effect could have contributed to differential prediction ability of calibration models, as mean age of the GOM Combined test set was 5 years old compared to

3 years old in the SA test set. Hence, using calibration models with similar age composition to targeted test sets may result in lower prediction error (Williams, 2013). Future investigation should further assess this phenomenon, as well as issues of rounding convention and regression effects, and explore potential mitigation techniques.

Spectral variation in red snapper otoliths older than 31 years of age was not modelled similarly to their younger counterparts, which might indicate further changes underlying otolith growth that affect FT-NIRS analysis at advanced fish age. That optimal cross-validation models used no preprocessing means there is no correction in spectral signatures for changing particle size or baseline correction for light scatter occurring due to size differences of the otoliths and their inherently different presentation on the sample window of the spectrometer. As such, it is possible that the SA Complete and All Regions Complete calibration models rely more on these physical otolith differences than other preprocessed models, in addition to any chemical differences. It is also possible that chemical changes underlying age prediction might taper off with age and/or size. These results suggest that multiple factors could affect spectral variation in thick, old otoliths, which has implications for their use with FT-NIRS applications.

This idea led us to evaluate the relationship of NIR light penetration with otolith size as a way of testing one of many potential sources of spectral variation. Size of red snapper otoliths range widely across age classes and are large relative to other fish species. Williams *et al.* (2015) demonstrated otolith thickness to be a diagnostic metric in morphometric indices for predicting otolith increment age in deepwater snappers and we found red snapper otolith thickness likewise to increase with age to a maximum of almost 6 mm in the oldest fish used in this study. Sample thickness alters NIR light penetration in cartilage at several wavenumber regions (Padalkar and Pleshko, 2015), and although the aragonite matrix of otoliths is less opaque and less proteinaceous than that of cartilage, the behaviour of light with the otolith organic matrix might be similar. Indeed, spectral differences between 6280 and 6080 cm^{-1} indicate that NIR light signal was attenuated in the oldest, thickest red snapper otolith, and additional regions of potential variation in spectral signature may exist that were not identified in our preliminary analysis. Thus, the effects of even gross otolith morphometrics on NIR light penetration and resulting spectral signatures are unknown and should be fully explored.

There is a great need for more understanding of how underlying otolith chemistry affects FT-NIRS age estimation to assess additional fine details of age prediction using FT-NIRS. Future otolith chemistry research should also consider adding FT-NIRS data collection to the methodology prior to additional destructive analyses, so that there are directly measured “wet chemistry” values for various constituents of interest to pair with spectral data for further investigation. Furthermore, standard operating procedures for spectral data collection and analysis must be developed to ensure that ages are predicted consistently and repeatably for each species should this technology be operationalized for management. A process for model updating will also need to be implemented to incorporate additional age-related uncertainty into spectral data to ensure continued prediction improvements. Given that the next US red snapper stock assessment is scheduled for 2021, it provides an important opportunity to develop

sensitivity analyses comparing the use of traditional and FT-NIRS ages in assessment models and resulting management benchmarks.

Supplementary data

Supplementary material is available at the ICESJMS online version of the manuscript.

Acknowledgements

The authors wish to thank the staff at the NMFS Southeast Fisheries Science Center Panama City Laboratory and the SC DNR Marine Resources Research Institute for providing age and other meristic data for this study, especially L. Thornton, N. Willett, D.B. White, J. Evans, and M. Willis. C. Kastle at the Alaska Fisheries Science Center and N. Earl, B. Robertory, and J. Weeks at the University of South Carolina provided assistance with FT-NIRS data collection. A. Andrews contributed valuable insights into otolith size and light penetration as it pertains to FT-NIRS age prediction. We also wish to thank J. Erickson for providing expertise on FT-NIRS equipment and light penetration experimental design. This work was supported by South Carolina Sea Grant [R/CF-23], an equipment grant from the College of Arts and Sciences, University of South Carolina, and funds from a SPARC Graduate Research and an ASPIRE-I grant from the Office of the Vice President for Research at the University of South Carolina. This is contribution # 826 of SCDNR's Marine Resources Research Institute. The findings and conclusions in the paper are those of the author(s) and do not necessarily represent the views of the National Marine Fisheries Service.

Data availability statement

The data underlying this article will be shared on reasonable request to the corresponding author.

References

- Allman, R., Barnett, B., Trowbridge, H., Goetz, L., and Evou, N. 2012. Red snapper (*Lutjanus campechanus*) otolith ageing summary for collection years 2009-2011. Sedar31-Dw05. Sedar, North Charleston, SC. 26 pp.
- Allman, R. J., Fitzhugh, G. R., Starzinger, K. J., and Farsky, R. A. 2005. Precision of age estimation in red snapper (*Lutjanus campechanus*). Fisheries Research, 73: 123–133.
- Allman, R. J., Lombardi-Carlson, L. A., Fitzhugh, G. R., and Fable, W. A. 2002. Age structure of red snapper (*Lutjanus campechanus*) in the Gulf of Mexico by fishing mode and region. Gulf and Caribbean Fisheries Institute, 53: 482–495.
- Andrews, A. H., Yeman, C., Welte, C., Hattendorf, B., Wacker, L., and Christl, M. 2019. Laser ablation accelerator mass spectrometry reveals complete bomb ^{14}C signal in an otolith with confirmation of 60-year longevity for red snapper (*Lutjanus campechanus*). Marine and Freshwater Research, 70: 1768–1780.
- Baker, S. J. M., and Wilson, C. A. 2001. Use of bomb radiocarbon to validate otolith section ages of red snapper *Lutjanus campechanus* from the northern Gulf of Mexico. Limnology and Oceanography, 46: 1819–1824.
- Barnett, B. K., Helser, T. E., Benson, I., Passerotti, M. S., and Erickson, J. 2019. Age prediction of Gulf of Mexico Red Snapper (*Lutjanus campechanus*) using near-infrared spectroscopy. In Proceedings of the Research Workshop on the Rapid Estimation of Fish Age Using Fourier Transform Near-Infrared Spectroscopy (FT-NIRS). Ed. by T. E. Helser, I. M. Benson, and B. K. Barnett. AFSC Processed Report 2019-06, 195 p. Alaska Fish. Sci. Cent., NOAA, Natl. Mar. Fish. Serv., 7600 Sand Point Way NE, Seattle, WA.

- Barnett, B. K., Patterson, W. F., Kellison, T., Garner, S. B., and Shiller, A. M. 2016. Potential sources of red snapper (*Lutjanus campechanus*) recruits estimated with Markov Chain Monte Carlo analysis of otolith chemical signatures. *Marine and Freshwater Research*, 67: 992–1001.
- Barnett, B. K., Thornton, L., Allman, R., Chanton, J. P., and Patterson, I. I. W. 2018. Linear decline in red snapper (*Lutjanus campechanus*) otolith ^{14}C extends the utility of the bomb radio-carbon chronometer for fish age validation in the Northern Gulf of Mexico. *ICES Journal of Marine Science*, 75: 1664–1671.
- Beamish, R. J., and Fournier, D. A. 1981. A method for comparing the precision of a set of age determinations. *Canadian Journal of Fisheries and Aquatic Sciences*, 38: 982–983.
- Campana, S. E. 1999. Chemistry and composition of fish otoliths: pathways, mechanisms and applications. *Marine Ecology Progress Series*, 188: 263–297.
- Campana, S. E. 2001. Accuracy, precision and quality control in age determination, including a review of the use and abuse of age validation methods. *Journal of Fish Biology*, 59: 197–242.
- Campana, S. E., and Thorrold, S. R. 2001. Otoliths, increments, and elements: keys to a comprehensive understanding of fish populations? *Canadian Journal of Fisheries and Aquatic Sciences*, 58: 30–38.
- Chen, J., and Wang, X. Z. 2001. A new approach to near-infrared spectral data analysis using independent component analysis. *Journal of Chemical Information and Computer Science*, 41: 992–1001.
- Couture, J. J., Singh, A., Rubert-Nason, K. F., Serbin, S. P., Lindroth, R. L., and Townsend, P. A. 2016. Spectroscopic determination of ecologically relevant plant metabolites. *Methods in Ecology and Evolution*, 7: 1402–1412.
- Cowan, J. H. Jr. 2011. Red snapper in the Gulf of Mexico and US South Atlantic: data, doubt, and debate. *Fisheries*, 36: 319–331.
- Helser, T. E., Benson, I., Erickson, J., Healy, J., Kastle, C., and Short, J. A. 2019a. A transformative approach to ageing fish otoliths using Fourier transform near infrared spectroscopy: a case study of eastern Bering Sea walleye pollock (*Gadus chalcogrammus*). *Canadian Journal of Fisheries and Aquatic Science*, 76: 780–789.
- Helser, T. E., Benson, I. M., and Barnett, B. K. (Ed.) 2019b. Proceedings of the Research Workshop on the Rapid Estimation of Fish Age Using Fourier Transform Near-Infrared Spectroscopy (FT-NIRS). AFSC Processed Report 2019-06, 195 p. Alaska Fisheries Science Center, NOAA, National Marine Fisheries Service, 7600 Sand Point Way NE, Seattle, WA.
- Izzo, C., Doubleday, Z. A., and Gillanders, B. M. 2016. Where do elements bind within the otoliths of fish? *Marine and Freshwater Research*, 67: 1072–1076.
- Lambert, B., Sikulu-Lord, M. T., Mayagaya, V. S., Devine, G., Dowell, F., and Churcher, T. S. 2018. Monitoring the age of mosquito populations using near-infrared spectroscopy. *Scientific Reports*, 8: 1–9.
- Limburg, K. E., and Elfman, M. 2017. Insights from two-dimensional mapping of otolith chemistry. *Journal of Fish Biology*, 90: 480–491.
- Lombardi, L. 2017. Summary of Red Snapper Age-Length Data by Data Providers for SEDAR52. SEDAR52-WP-14. SEDAR, North Charleston, SC. 24 pp.
- Manooch, C. S. III, and Potts, J. C. 1997. Age and growth of Red Snapper, *Lutjanus campechanus*, Lutjanidae, collected along the southeastern United States from North Carolina through the East Coast of Florida. *Journal of the Elisha Mitchell Scientific Society*, 113: 111–122.
- Mayagaya, V. S., Michel, K., Benedict, M. Q., Killeen, G. F., Wirtz, R. A., Ferguson, H. M., and Dowell, F. E. 2009. Non-destructive determination of age and species of *Anopheles gambiae* using near infrared spectroscopy. *The American Journal of Tropical Medicine and Hygiene*, 81: 622–630.
- Murray, I., and Williams, P. 1987. Chemical principles of near-infrared technology. In *Near Infrared Technology in the Agricultural and Food Industries*, pp. 29–31. Ed. P. Williams and K. Norris. American Association of Cereal Chemists, St. Paul, MN.
- Nelson, R. S., and Manooch, C. S. III, 1982. Growth and mortality of Red Snapper, *Lutjanus campechanus*, in the west central Atlantic Ocean and the northern Gulf of Mexico. *Transactions of the American Fisheries Society*, 111: 465–475.
- NMFS (National Marine Fisheries Service). 2018. Fisheries of the United States, 2017. U.S. Department of Commerce. NOAA Current Fishery Statistics No 2017. <https://www.fisheries.noaa.gov/feature-story/fisheries-united-states-2017> (last accessed 10 January 2020).
- Nowling, L., Gauldie, R. W., Cowan, J. H. Jr, and Carlo, E. D. 2011. Successful discrimination using otolith microchemistry among samples of red snapper *Lutjanus campechanus* from artificial reefs and samples of *L. campechanus* taken from nearby oil and gas platforms. *The Open Fish Science Journal*, 4: 1–9.
- Ogle, D. H., Wheeler P., and Dinno, A. 2018. FSA: Fisheries Stock Analysis. R package version 0.8.22. <https://github.com/droglenc/FSA> (last accessed 10 January 2020).
- Padalkar, M. V., and Pleshko, N. 2015. Wavelength-dependent penetration depth of near infrared radiation into cartilage. *Analyst*, 140: 2093–2100.
- Passerotti, M. S., Jones, C. M., Swanson, C. E., and Quattro, J. M. 2020. Fourier-transform near infrared spectroscopy (FT-NIRS) rapidly and non-destructively predicts daily age and growth in otoliths of juvenile red snapper *Lutjanus campechanus* (Poey, 1860). *Fisheries Research*, 223: 105439.
- Patterson, W. F. III, Cowan, J. H. Jr, Wilson, C. A., and Chen, Z. 2008. Temporal and spatial variability in juvenile red snapper otolith elemental signatures in the northern Gulf of Mexico. *Transactions of the American Fisheries Society*, 137: 521–532.
- Potts, J. (Ed.) 2009. Age Workshop for Red Snapper. SEDAR 24, Data Workshop, 10 August 2009.
- Reich, G. 2005. Near-infrared spectroscopy and imaging: basic principles and pharmaceutical applications. *Advanced Drug Delivery Reviews*, 57: 1109–1143.
- Rigby, C. L., Wedding, B. B., Grauf, S., and Simpfendorfer, C. A. 2014. The utility of near infrared spectroscopy for age estimation of deep water sharks. *Deep Sea Research. Part I*, 94: 184–194.
- Rigby, C. L., Wedding, B. B., Grauf, S., and Simpfendorfer, C. A. 2016. Novel method for shark age estimation using near infrared spectroscopy. *Marine and Freshwater Research*, 67: 537–545.
- Robins, J. B., Wedding, B. B., Wright, C., Grauf, S., Fowler, A., Saunders, T., and Newman, S. 2015. Revolutionising Fish Ageing: using Near Infrared Spectroscopy to Age Fish. State of Queensland through Department of Agriculture and Fisheries.
- SEDAR. 2008. SEDAR 15—Stock Assessment Report 1 (SAR 1)—South Atlantic Red Snapper. South East Data, Assessment, and Review. <https://sedarweb.org/docs/sar/S15%20SAR1RedSnap%20FINAL%20Revised%200309.pdf> (last accessed 10 January 2020).
- SEDAR. 2015. SEDAR Procedural Workshop 7: Data Best Practices. SEDAR, North Charleston SC. 151 pp.
- SEDAR. 2017. SEDAR 41—South Atlantic Red snapper Assessment Report—Revision 1. SEDAR, North Charleston, SC. 805 pp. <http://sedarweb.org/sedar-41> (last accessed 10 January 2020).
- SEDAR. 2018. SEDAR 52—Gulf of Mexico Red snapper Assessment Report. SEDAR, North Charleston, SC. 434 pp. http://sedarweb.org/docs/sar/S52_Final_SAR_v2.pdf.
- SEDAR. 2020. SEDAR 69—Atlantic Menhaden Stock Assessment Report. SEDAR, North Charleston, SC. 691 pp. <http://sedarweb.org/sedar-69> (last accessed 10 January 2020).

- SFB NMFS (Sustainable Fisheries Branch—National Marine Fisheries Service). 2015. Development of an Ageing Error Matrix for U.S. Red Snapper (*Lutjanus campechanus*). SEDAR41-DW48. SEDAR, North Charleston, SC. 8 pp.
- Sikulu-Lord, M. T., Maia, M. F., Milali, M. P., Henry, M., Mkandawile, G., Kho, E. A., Wirtz, R. A., *et al.* 2016. Near-infrared spectroscopy, a rapid method for predicting the age of male and female wild-type and Wolbachia infected *Aedes aegypti*. PLoS Neglected Tropical Diseases, 10: e0004759.
- Sluis, M. Z., Barnett, B. K., Patterson, W. F. III, Cowan, J. H. Jr, and Shiller, A. M. 2012. Discrimination of juvenile red snapper otolith chemical signatures from Gulf of Mexico nursery regions. Marine and Coastal Fisheries, 4: 587–598.
- Sluis, M. Z., Barnett, B. K., Patterson, W. F. III, Cowan, J. H. Jr, and Shiller, A. M. 2015. Application of otolith chemical signatures to estimate population connectivity of red snapper in the Western Gulf of Mexico. Marine and Coastal Fisheries, 7: 483–496.
- Sturrock, A. M., Hunter, E., Milton, J. A., Johnson, R. C., Waring, C. P., and Trueman, C. N. 2015. Quantifying physiological influences on otolith microchemistry. Methods in Ecology and Evolution, 6: 806–816.
- Thomas, O. R., Ganio, K., Roberts, B. R., and Swearer, S. E. 2017. Trace element–protein interactions in endolymph from the inner ear of fish: implications for environmental reconstructions using fish otolith chemistry. Metallomics, 9: 239–249.
- Thomas, O. R., and Swearer, S. E. 2019. Otolith biochemistry—a review. Reviews in Fisheries Science & Aquaculture, 27: 458–489.
- Tolleson, D. R., Randel, R. D., Stuth, J. W., and Neuendorff, D. A. 2005. Determination of sex and species in red and fallow deer by near infrared reflectance spectroscopy of the faeces. Small Ruminant Research, 57: 141–150.
- Vance, C. K., Kouba, A. J., and Willard, S. T. 2014. Near infrared spectroscopy applications in amphibian ecology and conservation: gender and species identification. NIR News, 25: 10–15.
- Vance, C. K., Tolleson, D. R., Kinoshita, K., Rodriguez, J., and Foley, W. J. 2016. Near infrared spectroscopy in wildlife and biodiversity. Journal of Near Infrared Spectroscopy, 24: 1–25.
- VanderKooy, S. (Ed.) 2009. A Practical Handbook for Determining the Ages of Gulf of Mexico Fishes, 2nd edn. Gulf States Marine Fisheries Commission, Publication No. 167, 136 p. Ocean Spring, MS.
- Vasconcelos-Filho, J. E., Thomsen, F. S. L., Stosic, B., Antonino, A. C. D., Duarte, D. A., Heck, R. J., Lessa, R. P. T., *et al.* 2019. Peeling the otolith of fish: optimal parameterization for micro-CT scanning. Frontiers in Marine Science, 6: 728.
- Wedding, B. B., Forrest, A. J., Wright, C., Grauf, S., Exley, P., and Poole, S. E. 2014. A novel method for the age estimation of Saddle tail snapper (*Lutjanus malabaricus*) using Fourier Transform-near infrared (FT-NIR) spectroscopy. Marine and Freshwater Research, 65: 894–900.
- White, D. B., and Palmer, S. M. 2004. Age, growth, and reproduction of the red snapper, *Lutjanus campechanus*, from the Atlantic waters of the southeastern US. Bulletin of Marine Science, 75: 335–360.
- Wiedower, E. E., Kouba, A. J., Vance, C. K., Hansen, R. L., Stuth, J. W., and Tolleson, D. R. 2012. Fecal near infrared spectroscopy to discriminate physiological status in giant pandas. PLoS One, 7: e38908.
- Williams, P. 2008. Near-Infrared Technology-Getting the Best Out of Light. A Short Course in the Practical Implementation of Near-Infrared Spectroscopy for the User. A Short Course Held in Conjunction with the 13th ANISG Conference. Australian Near Infrared Spectroscopy Group. Department of Primary Industries—Hamilton Centre, Victoria, Canada.
- Williams, P. 2013. Calibration development and evaluation methods B. Set-up and evaluation. NIR News, 24: 20–24.
- Williams, A. J., Newman, S. J., Wakefield, C. B., Bunel, M., Halafihi, T., Kaltavara, J., and Nicol, S. J. 2015. Evaluating the performance of otolith morphometrics in deriving age compositions and mortality rates for assessment of data-poor tropical fisheries. ICES Journal of Marine Science, 72: 2098–2109.
- Wilson, C. A., and Nieland, D. L. 2001. Age and growth of red snapper, *Lutjanus campechanus*, from the northern Gulf of Mexico off Louisiana. Fishery Bulletin, 99: 653–664.
- Wyanski, D.D.B., White, T., Smart, K., Kolmos, M. J. and Reichert, 2015. Marine Resources Monitoring, Assessment and Prediction Program: Report on Atlantic Red Snapper, *Lutjanus campechanus*, Life History for the SEDAR 41 Data Workshop. SEDAR41-DW35. SEDAR, North Charleston, SC. 39 pp.
- Zapp Sluis, M., Boswell, K. M., Chumchal, M. M., Wells, R. D., Soulen, B., and Cowan, J. H. Jr, 2013. Regional variation in mercury and stable isotopes of red snapper (*Lutjanus campechanus*) in the northern Gulf of Mexico, USA. Environmental Toxicology and Chemistry, 32: 434–441.

Handling editor: Alexander Arkhipkin